Separation Science and Technology
Publication details, including instructions for authors and subscription information:
http://www.informaworld.com/smpp/title~content=t713708471

Concentration Polarization Effects in the Use of Micellar-Enhanced Ultrafiltration to Remove Dissolved Organic Pollutants from Wastewater

Robert O. Dunn Jr.[a]; John F. Scamehorn[a]; Sherril D. Christian[b]
[a] School of Chemical Engineering and Materials Science and Institute for Applied Surfactant Research University of Oklahoma, Norman, Oklahoma [b] Department of Chemistry, Institute for Applied Surfactant Research University of Oklahoma, Norman, Oklahoma

To cite this Article Dunn Jr., Robert O. , Scamehorn, John F. and Christian, Sherril D.(1987) 'Concentration Polarization Effects in the Use of Micellar-Enhanced Ultrafiltration to Remove Dissolved Organic Pollutants from Wastewater', Separation Science and Technology, 22: 2, 763 — 789

To link to this Article: DOI: 10.1080/01496398708068980

URL: http://dx.doi.org/10.1080/01496398708068980

SEPARATION SCIENCE AND TECHNOLOGY, 22(2&3), 763-789, 1987

Concentration Polarization Effects in the Use of Micellar-Enhanced Ultrafiltration to Remove Dissolved Organic Pollutants from Wastewater

ROBERT O. DUNN, JR. and JOHN F. SCAMEHORN*

SCHOOL OF CHEMICAL ENGINEERING AND MATERIALS
SCIENCE AND INSTITUTE FOR APPLIED SURFACTANT
RESEARCH
UNIVERSITY OF OKLAHOMA
NORMAN, OKLAHOMA 73019

SHERRIL D. CHRISTIAN

DEPARTMENT OF CHEMISTRY AND INSTITUTE FOR APPLIED
SURFACTANT RESEARCH
UNIVERSITY OF OKLAHOMA
NORMAN, OKLAHOMA 73019

ABSTRACT

Micellar-enhanced ultrafiltration (MEUF) is used to remove 4-*tert*-butylphenol (TBP) from aqueous solution, a separation for which traditional ultrafiltration is ineffective. A micelle-forming surfactant is added to the solution. The micelles solubilize a high fraction of the TBP. The stream is then forced through an ultrafilter. Overall rejection of TBP was greater than 99% under all conditions studied and did not decrease with increasing pressure drop. Micelles were completely rejected by membranes with pore size 10 000 Dalton MWCO and below. Concentration polarization affects MEUF fluxes under conditions of interest. Gel polarization theory does not completely explain MEUF flux behavior. Selection of optimum operating parameters in MEUF application are discussed.

---

*To whom correspondence should be adressed

INTRODUCTION

Wastewater streams containing dissolved organics are a common problem in the chemical, petroleum, synfuels, and other industries. These organics are often toxic and must be removed before the water can be discharged to the environment or reused in the process. Ordinary ultrafiltration is ineffective in the removal of organic compounds with molecular weights below 300 Daltons (1). Alkylphenols are an example of a class of common pollutants with molecular weights often below this range.

Micellar-enhanced ultrafiltration (MEUF) is a recently developed technique (2,3) which can be used to remove soluble, low molecular weight organics from water, as illustrated schematically in Fig. 1. In this process, surfactant is added to the polluted aqueous stream. When the surfactant is present at concentrations greater than its critical micelle concentration (CMC), it forms aggregates called micelles, into which the organic pollutant solubilizes. The stream then passes through an ultrafiltration membrane with pore sizes small enough to block the micelles containing the solubilized organic pollutants. Since the micelles are fairly large (containing around 100 molecules for the surfactant used here), a membrane with a much larger pore size can be used to reject micelles than would be required to reject non-aggregated surfactant molecules. If the tendency for the pollutant to solubilize in the micelles is large, the concentration of unsolubilized organic in solution will be very small. The permeate solute concentration will approximately correspond to this unsolubilized solute concentration, resulting in a very pure permeate. If the retentate can be concentrated to high levels of surfactant and pollutant before concentration polarization or phase separation present operational difficulties, a high recycle ratio (permeate/feed) and a small waste stream containing the pollutant at high concentrations will result from the process.

In our previous study of MEUF (3), the removal of 4-*tert*-butylphenol (TBP) was studied using n-hexadecylpyridinium chloride (CPC) as the surfactant and a 1 000 Dalton molecular weight cut-off membrane with a constant transmembrane pressure drop of 414 kPa. In that work, the micelles were completely rejected, as long as high retentate surfactant concentrations (greater than approximately 225 mM CPC) were avoided. In the lower concentration region, rejections of 99.7%

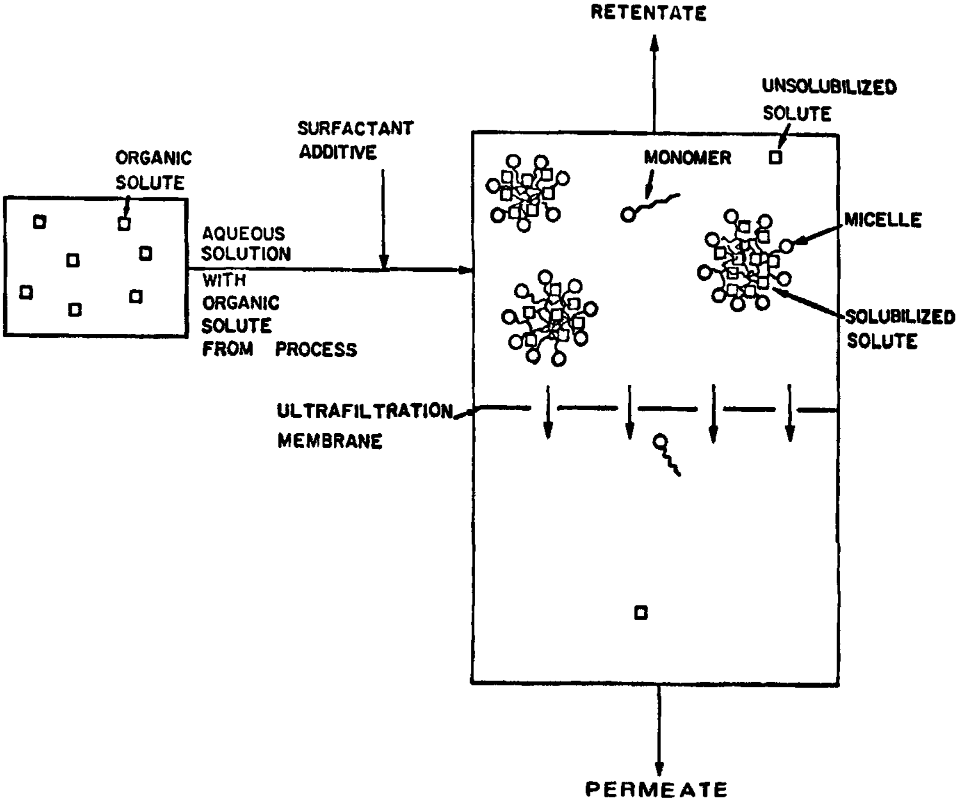

Fig. 1 Schematic of Micellar-Enhanced Ultrafiltration

for both TBP and CPC were observed and fluxes were only 30% below that of pure solvent (water).

This previous work established the feasibility of MEUF as a separation technique for TBP. In this paper, we examine the dynamics of the ultrafiltration process in much more detail. The effect of membrane pore size is determined and maximum feasible pore size and flux rate are established for the process. The effect of transmembrane pressure drop is then investigated. For the first time, the concentration polarization effects are quantified for MEUF. Considerations in the selection of optimum membrane and operating conditions for MEUF are discussed.

EXPERIMENTAL

The source and purification of materials used in this study, analysis of TBP and CPC and related techniques (changes are noted below) are described elsewhere (3).

The ultrafiltration experiments were carried out in Nuclepore 400 mL batch stirred cells. The membranes were 76 mm-diameter Nuclepore anisotropic cellulose acetate with an effective area of 30.2 cm^2. Molecular weight cut-offs used were 1 000, 5 000, 10 000, 20 000, and 50 000 Daltons. The membranes were pre-equilibrated by soaking them overnight in a solution containing 1.08 mM CPC and 0.108 mM TBP. This resulted in a quicker transition to steady state in experimental runs than the previously described method (3) of pre-soaking the membranes in feed solution. Feed solutions, arbitrarily prepared in a 10:1 ratio of CPC-to-TBP, of 300 mL were placed into the cell for each ultrafiltration run. All runs were made at 30°C with a stirrer speed of 845 RPM. Transmembrane pressure drops of 206, 310 and 414 kPa were used.

RESULTS

The thermodynamic phase boundaries (3) for the CPC-TBP system is shown in Fig. 2. The general retentate composition path for the ultrafiltration runs in this work is also shown; that is, the TBP vs. CPC concentrations in the retentate as a run progressed. From Fig. 2, the retentate was an isotropic solution under all conditions studied.

For practical MEUF use, surfactant would be introduced into the feed stream containing the dissolved organic solutes, and this stream would then be treated in a batch or continuous flow membrane device. In a batch operation, the retentate solution will become more concentrated in rejected species with increasing time as permeate is removed from the cell. In a continuous flow operation, the retentate solution will become more concentrated in rejected species with increasing distance (or residence time) through the device. For each configuration, it can be concluded that the retentate composition follows a path. A batch, stirred cell was used for this study. The resulting differential flux (or relative flux) and permeate concentration data, measured as functions of retentate

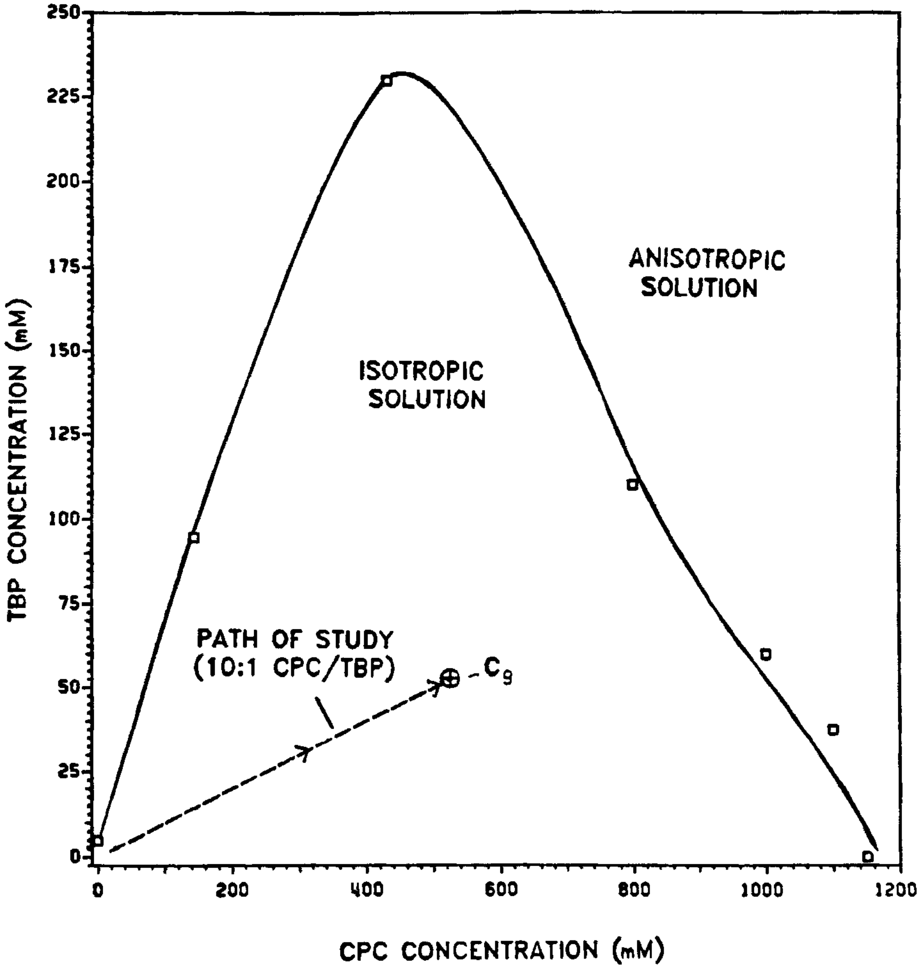

Fig. 2 CPC-TBP System Phase Boundary

concentration in the cell, can be integrated to predict the average flux and permeate concentrations for a continuous unit under specified conditions. Each of the runs in this work followed the same path, since the initial CPC/TBP concentration ratio was 10:1 for each run and rejection of both CPC and TBP were very close to 100% under all conditions studied. Given this, the retentate CPC/TBP concentration ratio is approximately constant at 10:1 under all conditions studied here, and the independent variable was chosen to be the retentate CPC concentration for data presentation.

The increase in retentate concentration in single batch experiments was limited, since vortices generated by the stirrer limited the fraction of solution which could permeate the membrane in the ultrafiltration run; therefore, several runs at different initial concentrations were made and then connected into a single path covering a much wider range of retentate compositions. It could be argued that the results may depend upon time of operation of the cell, as well as the condition of the retentate; that is, the boundary layer of fluid next to the membrane may take a long time to reach a steady state condition compared to the rate of change in the retentate solution. If this were the case, the batch cell results could not be used to predict performance in a continuous commercial device; however, as seen in Figs. 3, 4 and 5, the flux data for different ultrafiltration runs along a path form a continuous curve. For example, each path in Fig. 3 is composed of three separate runs. This indicates that the MEUF results depend only on the retentate properties and not the time of operation.

The base case for comparison is a 10 000 molecular weight cut-off (MWCO) membrane with a 414 kPa transmembrane pressure drop (ΔP). Complete permeate and retentate CPC and TBP concentrations, calculated apparent rejections, and relative fluxes are shown in Table 1 for the entire path studied. Relative fluxes were calculated as ratios of the absolute flux to corresponding fluxes of pure solvent water under identical flow conditions. Table 2 gives a list of pure water fluxes for each of the five membranes.

Absolute and relative fluxes for path runs through 1 000, 5 000, 10 000, 20 000, and 50 000 Dalton MWCO membranes with a ΔP of 414 kPa are presented in Figs. 3 and 4, respectively. Permeate compositions for CPC and TBP are plotted as a function of retentate CPC concentration in Figs. 6 and 7, respectively. Also shown in Fig. 6 are vapor pressure osmometry

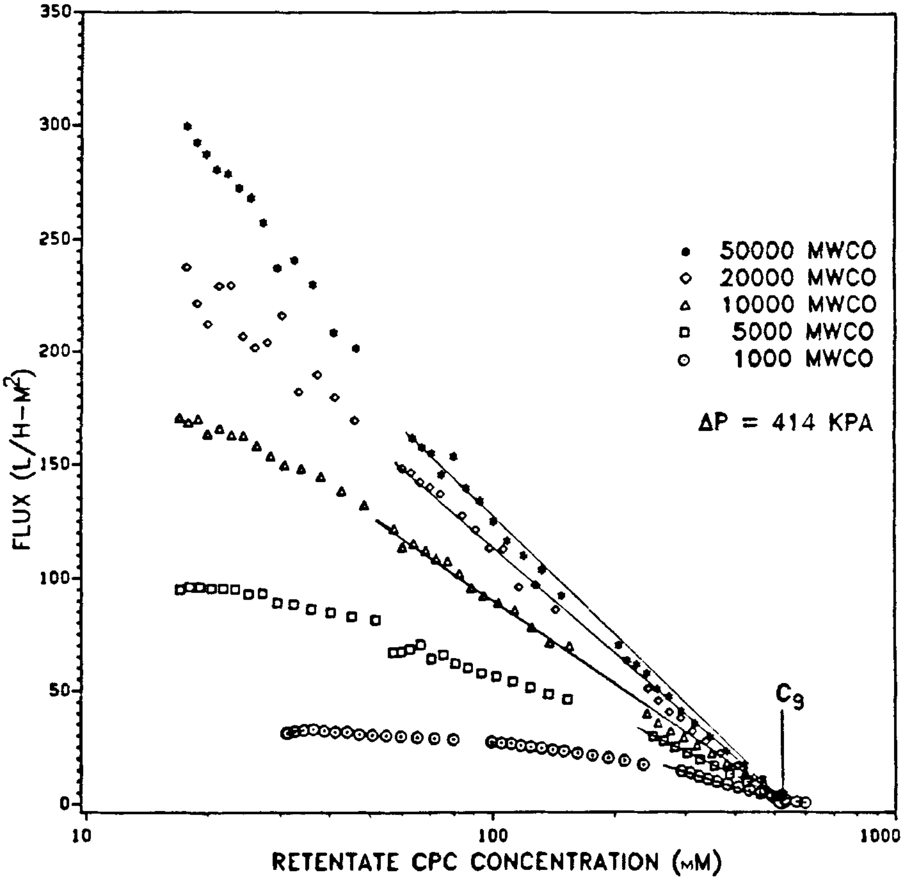

Fig. 3 Absolute Flux Rates for Various Membrane Pore Sizes

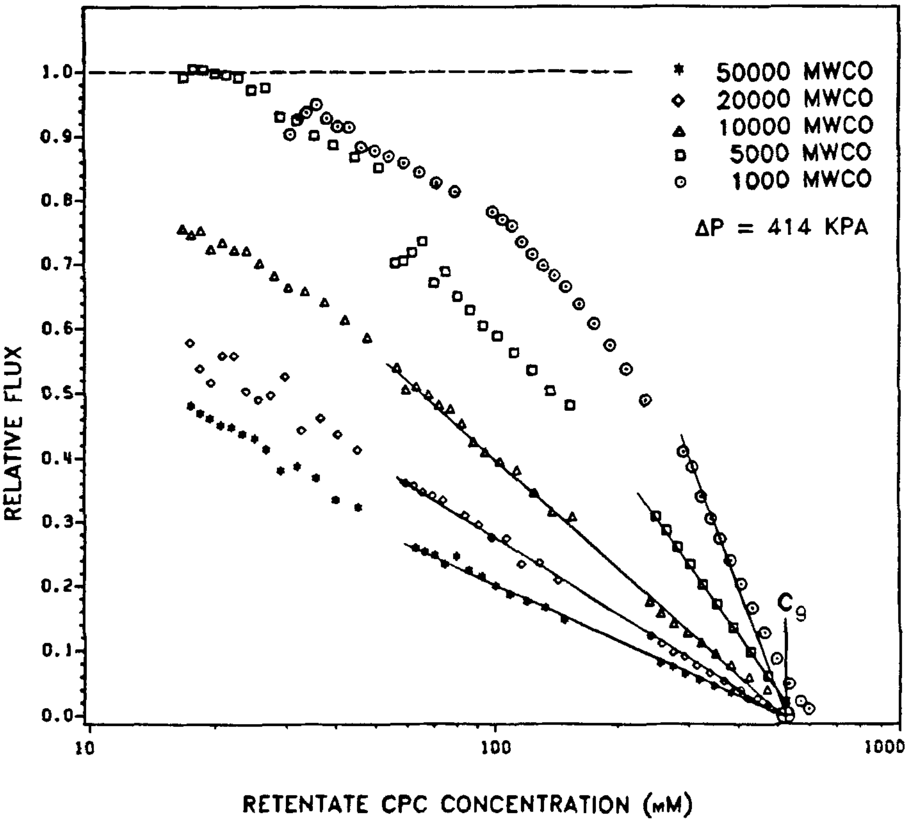

Fig. 4 Relative Flux Rates for Various Membrane Pore Sizes

measurements (3) for mean ionic molality of CPC, and in Fig. 7 are semi-equilibrium dialysis measurements (3) for unsolubilized TBP in the retentate.

The 10 000 MWCO membrane was chosen for detailed study of the effect of transmembrane pressure drop as representing a balance between flux reduction and solute rejection. Fig. 5 presents results for flux rates measured at ΔP values of 206 kPa, 310 kPa, and 414 kPa. Higher pressure drops were not studied to avoid membrane compression effects. Retentate CPC concentrations higher than the aforementioned 225 mM were not studied for the two lower pressure drops because MEUF is

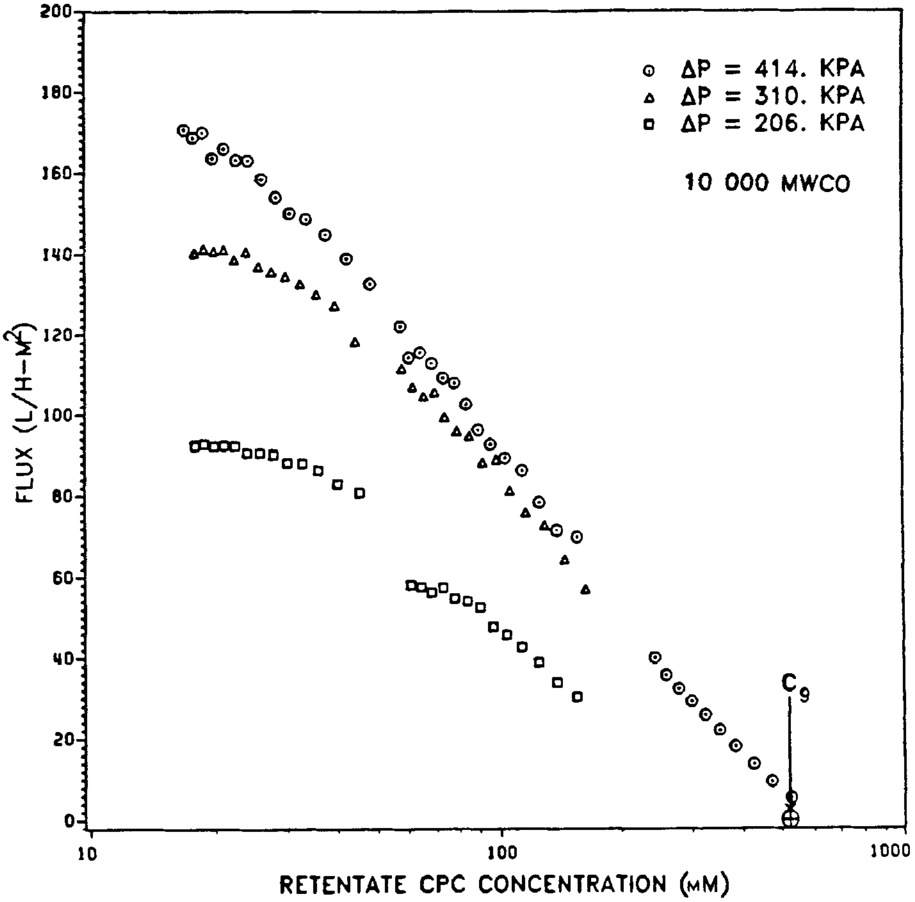

Fig. 5 Flux Rates for Various Transmembrane Pressure Drops

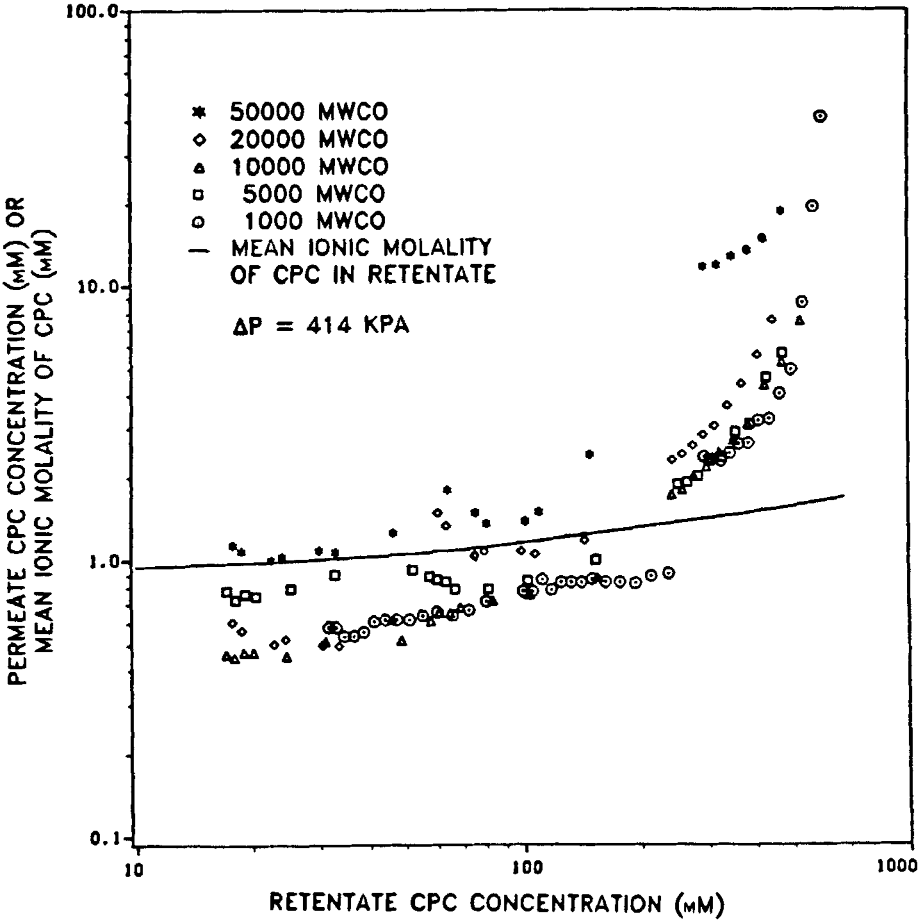

Fig. 6 Permeate CPC Concentrations and Mean Ionic Molality of CPC for Various Membrane Pore Sizes

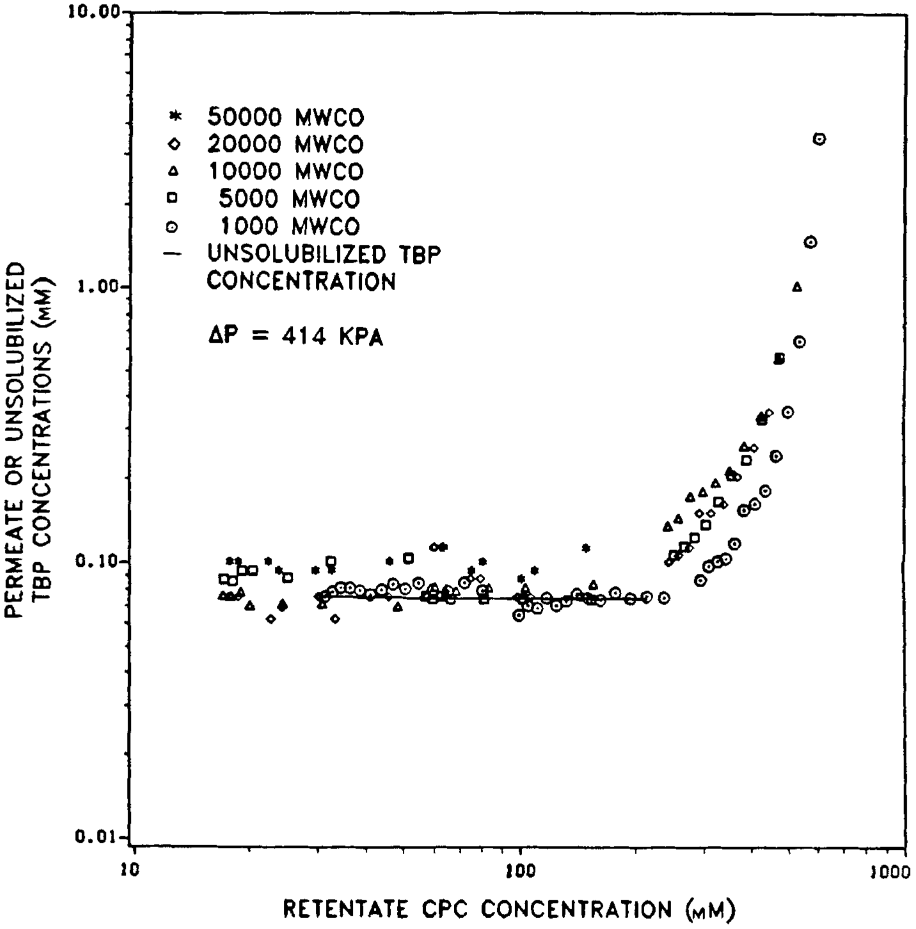

Fig. 7 Permeate and Unsolubilized TBP Concentrations for Various Membrane Pore Sizes

TABLE 1
Ultrafiltration Results: 10 000 MWCO Membrane and 414 kPa Transmembrane Pressure Drop

Concentrations (mM)				Rejection (%)		Fluxes	
Retentate		Permeate				Absolute $(L/H-M^2)$	Relative
CPC	TBP	CPC	TBP	CPC	TBP		
17.0	1.70	0.457	0.0763	97.31	95.51	171.	0.756
17.9	1.78	0.443	0.0759	97.52	95.82	169.	0.747
18.9	1.88	0.464	0.0784	97.56	95.83	170.	0.753
19.9	1.99	0.464	0.0704	97.67	96.46	164.	0.724
24.3	2.42	0.450	0.0715	98.15	97.04	163.	0.722
30.8	3.06	0.507	0.0714	98.35	97.66	150.	0.665
48.4	4.79	0.514	0.0698	98.94	98.54	133.	0.587
57.3	5.73	0.606	0.0766	98.94	98.66	122.	0.540
60.2	6.02	0.649	0.0821	98.92	98.64	114.	0.506
64.1	6.40	0.649	0.0784	98.99	98.78	115.	0.511
68.4	6.84	0.678	0.0795	99.01	98.84	113.	0.499
83.1	8.30	0.720	0.0819	99.13	99.01	103.	0.454
103.	10.3	0.749	0.0817	99.28	99.21	89.5	0.396
155.	15.5	0.862	0.0845	99.44	99.46	70.1	0.310
242.	24.2	1.74	0.137	99.28	99.43	40.0	0.177
258.	25.8	1.81	0.146	99.29	99.43	35.7	0.158
277.	27.7	2.03	0.175	99.27	99.37	32.3	0.143
299.	29.9	2.19	0.182	99.27	99.39	29.2	0.129
323.	32.3	2.47	0.196	99.23	99.39	25.8	0.114
350.	35.1	2.74	0.217	99.22	99.38	22.0	0.0972
383.	38.4	3.12	0.268	99.18	99.30	18.0	0.0795
424.	42.5	4.32	0.345	98.18	99.19	13.6	0.0601
471.	47.2	5.24	0.561	98.89	98.81	9.36	0.0414
526.	52.6	7.38	1.03	98.60	98.04	5.31	0.0235

TABLE 2
Pure Solvent Flux Rates

Membrane Pore Size (MWCO)	Flux $(L/H-M^2)$
1 000.	34.5
5 000.	95.8
10 000.	226.
20 000.	411.
50 000.	622.

ineffective beyond this limit. The effect of ΔP on flux at constant retentate CPC concentrations is shown in Fig. 8. Permeate CPC and TBP concentrations for these lower pressure drop runs are presented in Figs. 9 and 10, respectively.

DISCUSSION

Fluxes

For any type of pressure filtration, the absolute flux can be related to resistances to flow and ΔP through the following relation (1):

$$J_w = \Delta P/(R_c+R_m) \qquad (1)$$

where J_w is the solvent (water) flux at 100% solute rejection (a condition which is nearly satisfied under all conditions studied here), R_m is the resistance to flow caused by the membrane, and R_c is the resistance to flow (if any) within the hydrodynamic boundary layer next to the membrane.

In the ultrafiltration of a very dilute solution, or when using a ultrafiltration membrane with small enough pore sizes, the membrane resistance will dominate ($R_m>>R_c$); therefore, J_w becomes a linear function of ΔP (1). For example, from Fig. 8, the flux is proportional to ΔP for pure water for a 10 000 MWCO membrane. From Fig. 3, fluxes for MEUF are nearly equal to pure solvent fluxes for membranes of 1 000 and 5 000 MWCO when the retentate CPC concentration is less than about 25 mM. From Fig. 5, for a 10 000 MWCO membrane with ΔP values of 206 kPa and 310 kPa, the fluxes are only slightly dependent on concentration in the lower concentration region of the path; therefore, the absolute flux approaches the solvent flux and is nearly proportional to pressure drop, at low concentrations and ΔP values, as seen in Fig. 8.

As the retentate becomes more concentrated along any given path, the solution will enter the concentration polarization regime. In this regime, a "hydrodynamic boundary layer" forms near the membrane surface, and contains a higher concentration of rejected species than the bulk solution. As the retentate becomes more concentrated, or the applied ΔP is increased, the contribution of the boundary layer to the total resistance becomes more significant. As a result, the relative flux declines from unity. Increasing the

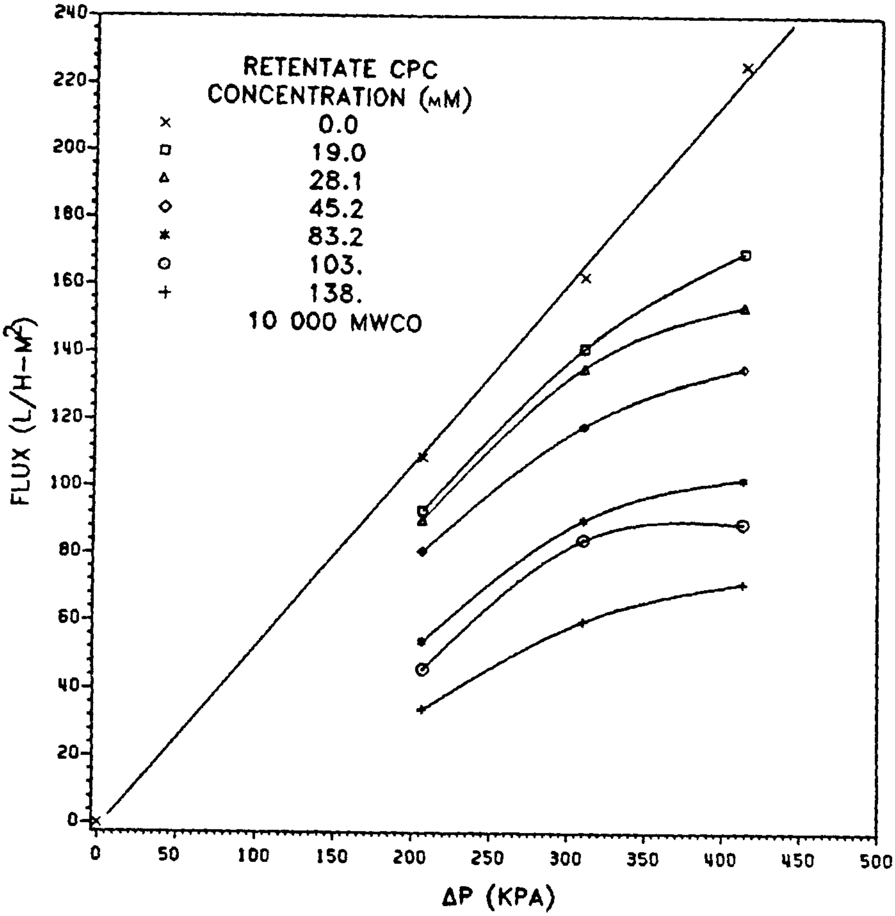

Fig. 8 Permeate Fluxes as a Function of Transmembrane Pressure Drop at Constant Retentate CPC Concentrations

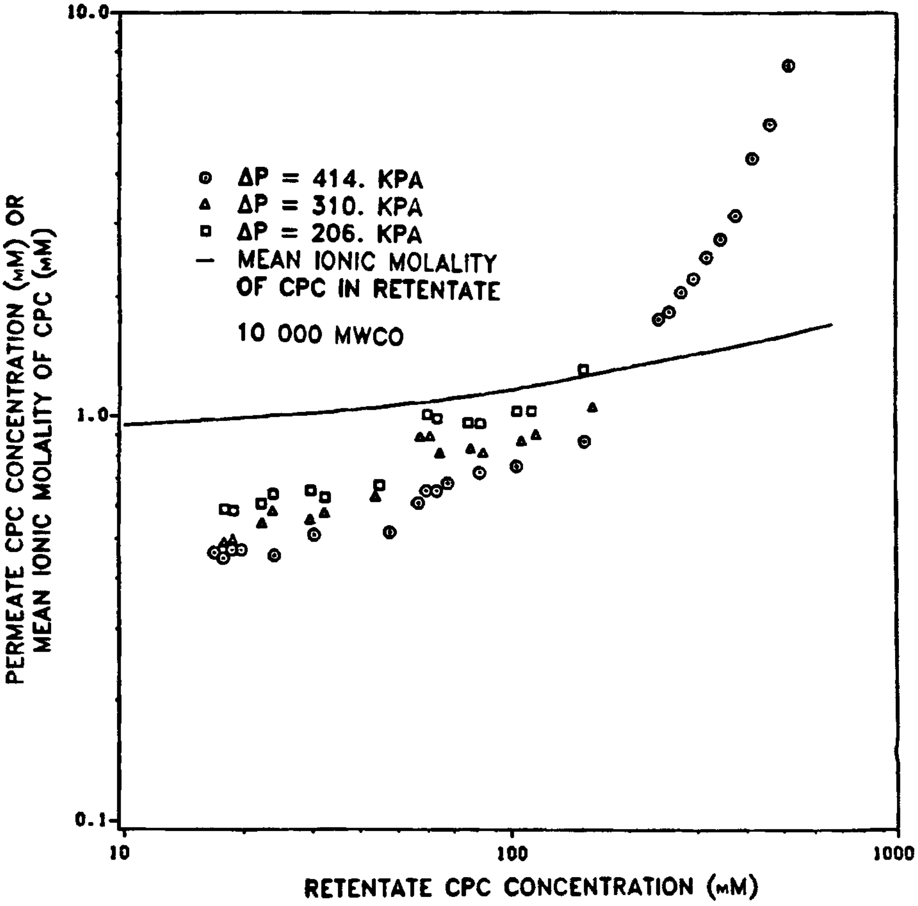

Fig. 9 Permeate CPC Concentrations and Mean Ionic Molality of CPC for Various Transmembrane Pressure Drops

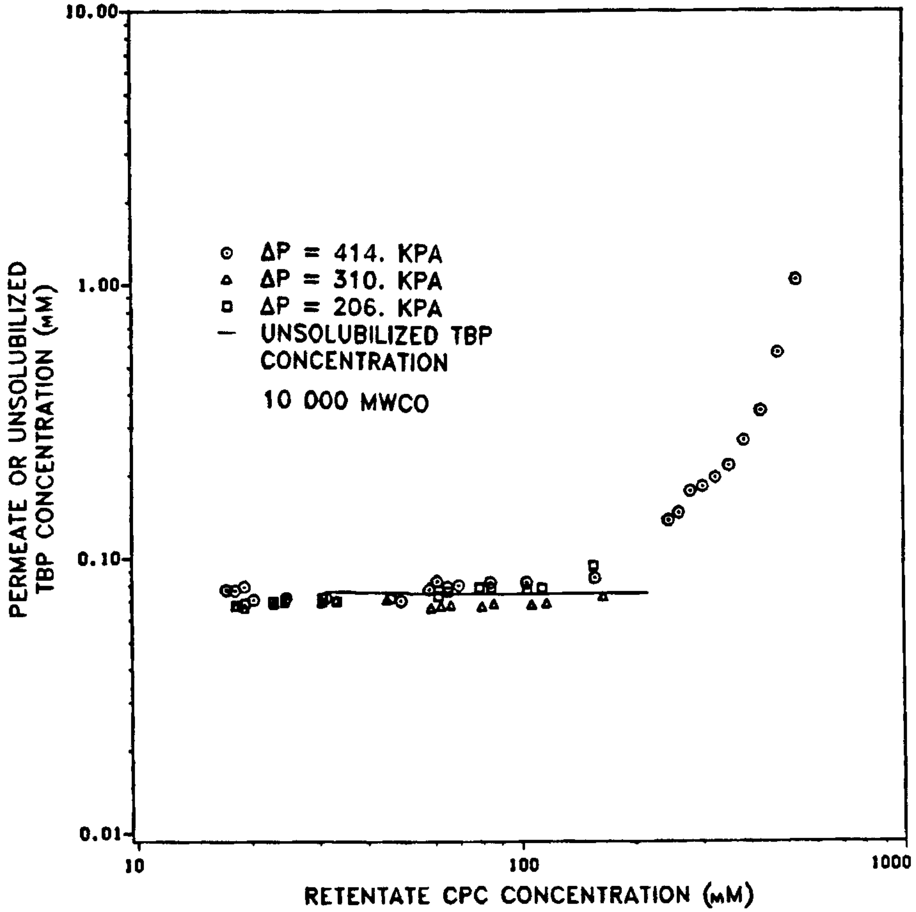

Fig. 10 Permeate and Unsolubilized TBP Concentrations for Various Transmembrane Pressure Drops

membrane pore size decreases the relative contribution of the membrane resistance (1); therefore, the relative contribution of the boundary layer resistance becomes more significant. The decrease in the permeate fluxes caused by concentration polarization can be seen in Figs. 3 and 4, for the varying membrane pore size experiments. This effect can also be seen in Figs. 5 and 8 where, except for pure water, the flux does not increase proportionally with increasing ΔP, as R_c in Equation (1) becomes increasingly significant. For the system studied here, MEUF is generally in the concentration polarization regime for operating conditions of interest.

When the retentate is further concentrated into the concentration polarization regime, the resistance term in Equation (1) may become dominated by R_c. In the gel polarization model (1,4,5), the concentration of solute at or near the membrane surface increases until it reaches a maximum value, commonly referred to as the gel concentration (C_g) (1,4-6). According to gel polarization theory, C_g is independent of the bulk concentration, the applied ΔP, the flow conditions, and the membrane characteristics (1,4). At this point, the solute forms a thixotropic gel adjacent to the membrane analogous to cake formation in ordinary filtration (1). Fig. 11 presents a schematic of the gel layer with respect to the hydrodynamic boundary layer. When the solution is in the gel polarization regime, and the boundary layer is considered to be at steady state (the convective mass transport of the solute to the membrane surface just equals the back-diffusive from the membrane caused by the associated concentration gradient), the flux will vary with the bulk concentration (C_b) as follows:

$$J_w = K[\ln(C_g/C_b)] \tag{2}$$

where K is the mass transfer coefficient. According to Equation (2), when the solution concentration is equal to the gel concentration, the flux is zero. A plot of the absolute (or relative) flux vs. $\ln(C_b)$ should be linear with the slope indicating the value of K. Figs. 3 and 4 indicate that Equation (2) is obeyed for each membrane used, as the relative fluxes approached zero.

As shown in Figs. 3 and 4, and in Table 3, approximately the same gel concentration is observed for each pore size, with an average value of 528 mM CPC and 52.9 mM TBP. This gel point is shown in relation to the phase boundaries in Fig. 2. The gel point is not close

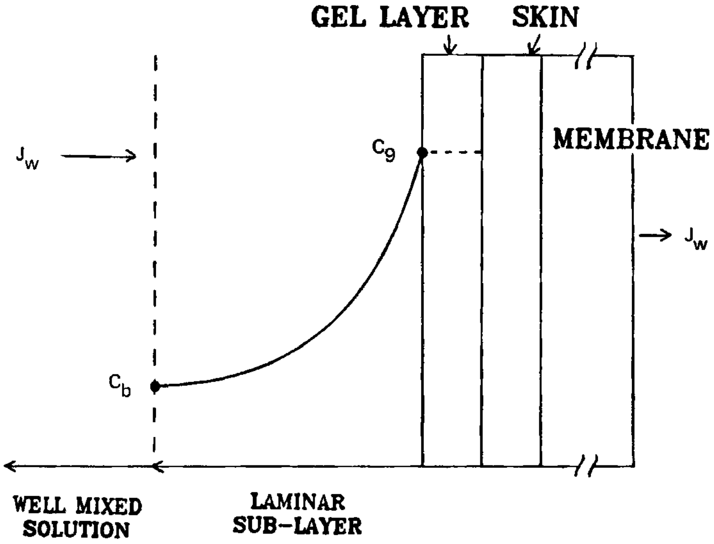

Fig. 11 Schematic of Boundary Layer and Gel Layer Formation in Ultrafiltration

TABLE 3

Gel Concentrations and Mass Transfer Coefficients

Membrane Pore Size (MWCO)	ΔP (kPa)	C_g (mM) CPC	TBP	K (L/H-M^2)
1 000.	414.	524.	52.6	25.
5 000.	414.	548.	55.0	38.0
10 000.	414.	523.	52.4	55.3
20 000.	414.	521.	52.4	65.
50 000.	414.	522.	52.3	74.1

to any thermodynamic phase boundary; therefore, the gel which forms on the membrane surface is not a result of phase separation. It has been shown, in addition, that the solution at this gel concentration is very viscous (about 6 cP (3)).

Consider the flux data given in Figs. 5 and 8. While the flux is nearly proportional to the pressure drop for the paths run at ΔP values of 206 kPa and 310 kPa, the flux increases only slightly between paths run at ΔP values of 310 kPa and 414 kPa. From Fig. 5, the data for the three paths at different transmembrane pressure drops all extrapolate approximately to the corresponding gel concentration inferred from Figs. 3 and 4. Also, the same gel concentration is observed when the stirrer speed (shear forces) is varied for this same system (7).

The data in Fig. 3 and 4 illustrate that the concentration range, between the point where concentration polarization begins and the gel point, increases as the membrane pore size increases. Also, the point where the flux seems to become a linear function of $\ln(C_b)$ occurs at lower retentate concentrations as the membrane pore size increases; that is, the point where the gel initially forms occurs at lower retentate concentrations as the membrane pore size is increased. Apparently, gel layer formation removes some of the advantage of using higher MWCO membranes. The ratio of the fluxes for two membranes of increasing MWCO at a specific condition in a MEUF application is not as great as the ratio of the fluxes for pure solvent for those same membranes; that is, the relative flux is lower for higher MWCO membranes, as seen in Fig. 4.

Fig. 12 and Table 3 give mass transfer coefficients calculated for each membrane (MWCO) from the data given in Fig. 3 and from Equation (2). The value of K increases in direct contradiction with gel polarization theory. Since the gel concentration is independent of membrane permeability, and the mass transfer coefficient can only be a function of the shear rate at the membrane surface, the cell geometry, and the solute diffusivity; then according to Equation (2), the permeate flux must be independent of the membrane permeability (1,4). The data in Figs. 3 and 4 indicate that C_g is independent of membrane pore size, but the corresponding K values are not. This pattern is very significant for the lower membrane pore sizes.

When the gel layer is formed, the flux should become invariant with increasing ΔP; however, from

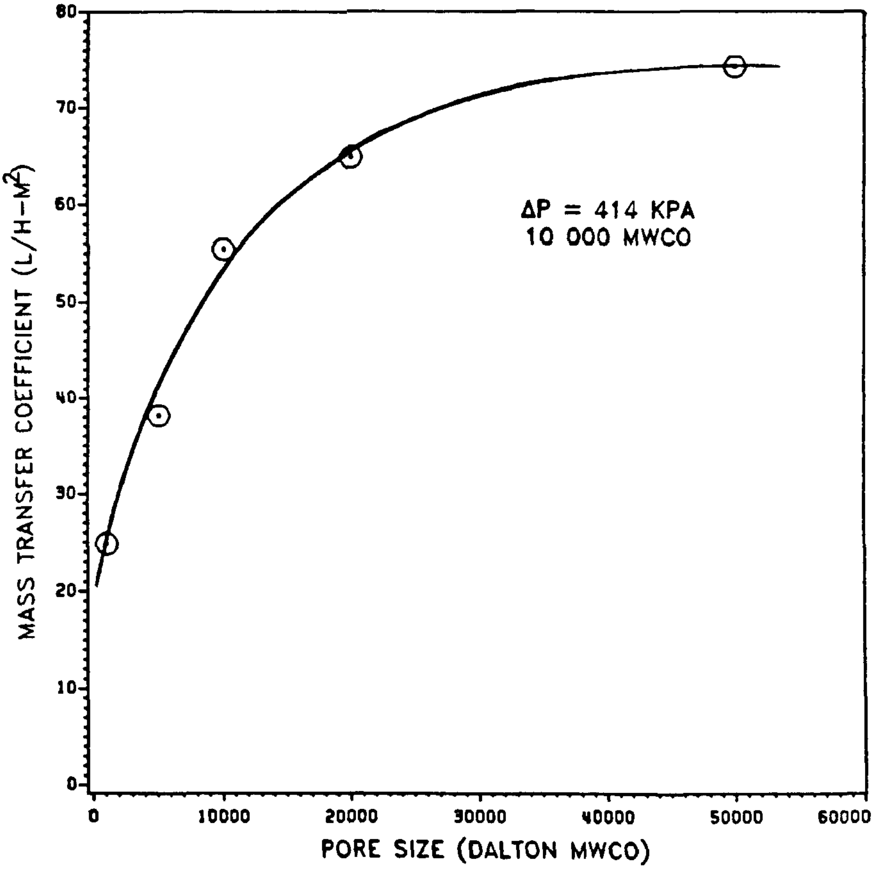

Fig. 12 Mass Transfer Coefficient as a Function of Membrane Pore Size

Fig. 5, the flux data for a ΔP of 310 kPa varies linearly with the log of the retentate CPC concentration, indicating that some type of gel layer has formed at this pressure drop. But, the flux increases slightly as the ΔP is increased to 414 kPa. Increasing flux with increasing ΔP at gel layer conditions has been previously observed in ultrafiltration (6).

In our previous work (3), we observed that the fluxes were essentially independent of stirrer speed at concentrations which we have found to be in the concentration polarization regime in this work. From that result, we incorrectly concluded that we did not have concentration polarization under the conditions used there. The relative independence of the flux on the shear rate (under some conditions) when concentration polarization is present is yet another unusual characteristic of MEUF. For MEUF in general, the boundary layer and the membrane characteristics affect the fluxes in any portion of the concentration polarization regime. Formation of some type of flux hindering gel adjacent to the membrane surface explains why some of the advantages of using more porous membranes are lost. Finally, due to contradictions in flux behavior and the apparent dependency of the mass transfer coefficient on membrane permeability, it can be concluded that the gel polarization model does not satisfactorily explain the behavior of MEUF in advanced stages of concentration polarization.

Permeate Purity

Consider the CPC concentrations in the permeate in Fig. 6 below a retentate CPC concentration of 225 mM. For the 1 000 MWCO membrane, the CPC concentration is below the mean ionic molality of CPC in the retentate, a concentration which would be expected to approximate the permeate CPC concentration if micelles were completely rejected and monomer hindrance were negligible (3). For the 5 000 MWCO membrane, the CPC concentration is somewhat higher than for the 1 000 MWCO membrane. This may be due to the monomer being less hindered during passage through larger pores. The 10 000 MWCO membrane exhibits a lower permeate CPC concentration than the 5 000 MWCO membrane. This effect may be due to an earlier development of the concentration polarization regime for the former, as seen in Fig. 4. The boundary layer, containing an increased rejected species concentration, acts as a presieve to aid the membrane in rejecting solute (1). Larger particles in the boundary layer (in our case, micelles) are known to presieve smaller particles (in our case, monomer) (1). For the 10 000 MWCO membrane, this effect counteracts the reduced monomer hindrance.

The 20 000 and 50 000 MWCO membranes produce permeate CPC concentrations which are around or above the mean ionic molality and substantially above the 1 000 and 10 000 MWCO membrane data. Some micelles are leaking through the membrane for these higher pore sizes. Still, it is remarkable that the vast majority of micelles are being rejected for such a large membrane pore size. If a micelle is being forced through a pore smaller than its minimum diameter by solvent flux, rather than deform, it may disassociate to form monomer which will rapidly diffuse away from the membrane and reform a micelle in the bulk retentate solution. Only pores large enough to let micelles permeate relatively unhindered will allow micelle leakage. This is a valuable characteristic for MEUF from a practical viewpoint.

Consider now the TBP concentrations in the permeate in Fig. 7 below a retentate CPC concentration of about 225 mM. The same trend is seen with increasing membrane pore size as for the aforementioned CPC data, but in this case, the 1 000, 5 000, and 10 000 MWCO membranes permeate TBP concentration results approximately correspond to the unsolubilized TBP concentrations in the retentate. The permeate TBP concentrations for the 20 000 and 50 000 MWCO data are above this level. This substantiates that an insignificant level of micelle leakage occurs for MWCO membranes of 10 000 and below. Some micelle leakage occurs for MWCO levels of 20 000 and above. From a comparison of the 1 000, 5 000, and 10 000 MWCO membrane data, the concentration polarization boundary layer presieving effect may improve rejections of TBP, as well as CPC, but not as extensively. When small enough pore sizes are selected such that micelles are rejected, others have observed solute concentrations in the permeate being equal to unsolubilized concentrations in the retentate (8,9). Our laboratory has discovered that this is also valid for MEUF of n-alcohols using CPC (10).

From the discussion of the flux rate data, we concluded that concentration polarization is present for almost all runs just discussed; yet, almost no decrease in rejection is observed as concentration polarization becomes further pronounced. This is a valuable aspect of MEUF, since quite high rejections are attainable at high fluxes.

Consider the retentate CPC concentrations above 225 mM in Figs. 6 and 7. Both CPC and TBP permeate concentrations increase rapidly with retentate concentrations in this region. This has been previously attributed to passage of n-mers (for example, dimers, trimers, and etc.) through the membrane (3). The data in Figs. 6 and 7 can be explained on this basis with the additional consideration of micelle leakage for large MWCO membranes. From a practical standpoint, this high concentration region should be avoided for any membrane pore size. This imposes a limit on recycle ratios (permeate/feed ratios), but the undesirable concentrations are so high that this limitation is not severe.

The effect of ΔP on permeate purity in Figs. 9 and 10 only considers the region of the low retentate concentrations which are feasible for effective separation. The permeate CPC concentration decreases as the ΔP (and the flux) increases. This is due to the higher degree of concentration polarization under higher ΔP conditions, increasing the presieving effect for surfactant monomer. At very low values of ΔP, other authors have observed that the surfactant concentration in the permeate is equal to the mean ionic molality of surfactant in the retentate (11). In contrast to the CPC, the hindrance of the unassociated TBP is negligible, so it is nearly at an equilibrium concentration in the permeate. As shown in Fig. 10, the ΔP has little effect on the permeate TBP concentration. At all ΔP values studied, no micelle leakage was observed for the 10 000 MWCO membrane.

From Figs. 7 and 10, as long as membrane pore sizes no greater than 10 000 MWCO are used, and high surfactant concentrations are avoided, the permeate TBP concentration is very nearly at its equilibrium unsolubilized concentration in the retentate; therefore, in order to predict the performance of MEUF with respect to rejection of the pollutant, MEUF experiments need not be run. Equilibrium methods such as semi-equilibrium dialysis (12) can predict performance. The maximum surfactant concentration in the permeate under these conditions can be estimated by the mean ionic molality, which can be approximated by the CMC, an easily measured quantity. This can potentially simplify screening for new potential pollutants to be removed from wastewater streams. MEUF data must be available to predict flux values, and scale-up of work such as that done here to commercial hollow-fiber, spiral-wound, and other units should allow development of such information for general application. As group contribution methods of predicting solubilization behavior of various organics are developed, the ability to estimate performance of MEUF on an a priori basis should be attainable. This is a goal of our current research.

SUMMARY OF PERFORMANCE OF MEUF

This section discusses the selection of optimum conditions for application of MEUF for removal of TBP from wastewater streams.

Increasing ΔP resulted in no deleterious effects on flux or permeate purity. Of course, pressures high enough to cause membrane compression should be avoided, but within this constraint, as high a ΔP value as possible should be used to minimize membrane area requirements.

In order to compare the effect of membrane pore size, the data presented in this paper were analyzed for a feed being treated from an initial composition of about 17 mM CPC and 1.7 mM TBP to a final retentate composition of 225 mM CPC and 22.5 mM TBP with a ΔP of 414 kPa. This path is illustrated in Fig. 2, although the path was not followed to the gel point. The undesirable high CPC concentrations above 225 mM which have been discussed were avoided in this path. The overall permeate composition, membrane area required per unit flow rate of solution treated, and the product permeate to feed ratio are reported in Table 4.

As membrane pore size is increased, membrane area requirements decrease due to greater flux. The rejections of CPC and TBP are maximized for the 1 000 and 10 000 MWCO membranes. At larger pore sizes, rejections decrease. Recycle (permeate/feed) ratios are a respectable 92.6% for all cases.

It is interesting to observe the trade-offs of increasing membrane pore size. When increasing pore size from 1 000 to 10 000, the membrane area decreases by 76%; therefore, only 24% of the membrane area reported in our previous paper (where only 1 000 MWCO membranes were studied) need be used when employing a 10 000 MWCO membrane with no deterioration in rejections. When the pore size is increased from 10 000 to 20 000 MWCO, the membrane area decreases by 20%, while the TBP and CPC rejections decrease slightly. When increasing pore size from 20 000 to 50 000 MWCO, the membrane area decreases by 12%, while the rejections of both TBP and CPC decrease, but still remained greater than 99% for the most porous membrane studied.

The CMC of CPC does provide an upper limit on permeate CPC concentrations (about 0.88 mM (13)) except for case of the 50 000 MWCO membrane, where substantial micelle leakage occurs.

The optimum pore size membrane for use in MEUF will still depend on how pure the permeate must be in specific application. From this analysis, one can conclude that despite slight micelle leakage, MWCO

TABLE 4

Summary of Performance of MEUF for Treatment of a Process Stream for Various Membrane Pore Sizes

Membrane (MWCO)	Feed (mM)		Overall Permeate (mM)		Final Retentate (mM)		Overall Rejection (%)		Membrane Area ($M^2/L/H$)	Permeate/Feed Ratio (L/L)
	CPC	TBP	CPC	TBP	CPC	TBP	CPC	TBP		
1 000	16.6	1.63	.638	.0792	225.	22.5	99.72	99.65	0.0423	0.926
5 000	16.6	1.66	.726	.0881	225.	22.5	99.68	99.61	0.0184	0.926
10 000	16.6	1.66	.56	.0755	225.	22.5	99.75	99.66	0.0121	0.926
20 000	17.2	1.72	.69	.0771	225.	22.5	99.69	99.66	0.00968	0.926
50 000	17.2	1.72	1.33	.101	225.	22.5	99.41	99.55	0.00850	0.926

values of 20 000 and 50 000 and perhaps even higher result in extremely good rejection characteristics with minimum membrane area requirements and minimum capital cost.

ACKNOWLEDGEMENTS

Financial support for this work was provided by the following organizations: The Office of Basic Energy Sciences of the Department of Energy - Contract DE-AS05-84ER13175, the University of Oklahoma Energy Resources Institute, and the Oklahoma Mining and Minerals Resources Research Institute. N-hexacdecylpyridinium chloride (CPC) was contributed by Hexcel Corporation. Assistance was provided by George A. Smith and L. Lane Gibbs.

REFERENCES

1. M. C. Porter, in Handbook of Separation Techniques for Chemical Engineers, McGraw-Hill, New York, 1979, Section 2.1.
2. P. S. Leung, in Ultrafiltration Membranes and Applications (A. R. Cooper, ed.), Plenum, New York, 1979, 415.
3. R. O. Dunn,Jr., J.F. Scamehorn, and S. D. Christian, Sep. Sci. Tech., 20, 257 (1985).
4. H. K. Londsdale, J. Memb. Sci., 10, 81 (1981).
5. A. S. Michaels, Chem. Engr. Prog., 64, 31 (1968).
6. M. S. Le, and J.A. Howell, Chem. Eng. Res. Des., 62, 373 (1984).
7. R. O. Dunn,Jr., Ph. D. Dissertation, University of Oklahoma, In Preparation.
8. A. E. Aboutaleb, A. M. Sakr, H. M. El-Sabbagh, and S. I. Abdelrahman, Pharm. Ind., 42, 940 (1980).
9. A. E. Aboutaleb, A. M. Sakr, H. M. El-Sabbagh, and S. I. Abdelrahman, Arch. Pharm. Chem. Sci. Ed., 5, 105 (1977).
10. L. L. Gibbs, J. F. Scamehorn, and S. D. Christian, J. Memb. Sci., submitted.

11. I. W. Osborne-Lee, R. S. Schecter, and W. H. Wade, J. Colloid Interface Sci., 94, 179 (1983).

12. S. D. Christian, G. A. Smith, E. E. Tucker, and J.F. Scamehorn, Langmuir, 1, 564 (1985).

13. J. F. Rathman, and J. F. Scamehorn, J. Phys. Chem., 88, 5807 (1984).